

# RSC Advances



This is an *Accepted Manuscript*, which has been through the Royal Society of Chemistry peer review process and has been accepted for publication.

*Accepted Manuscripts* are published online shortly after acceptance, before technical editing, formatting and proof reading. Using this free service, authors can make their results available to the community, in citable form, before we publish the edited article. This *Accepted Manuscript* will be replaced by the edited, formatted and paginated article as soon as this is available.

You can find more information about *Accepted Manuscripts* in the [Information for Authors](#).

Please note that technical editing may introduce minor changes to the text and/or graphics, which may alter content. The journal's standard [Terms & Conditions](#) and the [Ethical guidelines](#) still apply. In no event shall the Royal Society of Chemistry be held responsible for any errors or omissions in this *Accepted Manuscript* or any consequences arising from the use of any information it contains.



## Glycosylation improves the functional characteristics of chlorogenic acid-lactoferrin conjugates

Received 00th January 20xx,

Fuguo Liu,<sup>a</sup> Cuixia Sun,<sup>a</sup> Di Wang,<sup>a</sup> Fang Yuan<sup>a</sup> and Yanxiang Gao\*<sup>a</sup>

Accepted 00th January 20xx

DOI: 10.1039/x0xx00000x

www.rsc.org/

In the present study, chlorogenic acid (CA)-lactoferrin (LF) conjugate prepared via alkali treatment was glycosylated with glucose (Glc) and polydextrose (PD) by Maillard reaction. Formation of the covalent CA-LF-Glc/PD ternary conjugates was confirmed by matrix-assisted laser desorption/ionization time-of-flight mass spectrometry (MALDI-TOF-MS), Fourier transform infrared (FTIR) spectroscopy, differential scanning calorimetry (DSC) and fluorescence analyses. The results showed that the grafting ratio between CA-LF conjugate and Glc/PD was 40.50% for CA-LF-Glc ternary conjugate and 11.72% for CA-LF-PD ternary conjugate. Conjugating CA and Glc/PD onto LF changed the conformation of the protein, leading to a reduction in the  $\alpha$ -helix content and an increase in unordered structure. The thermal stability of CA-LF conjugate was remarkably improved by Maillard-type conjugation. According to AFM and DLS results, the ternary conjugates showed coarser structure and bigger particles size than their mixtures. The reducing power effect was increased from 206.91  $\mu\text{mol Trolox/g}$  of CA-LF conjugate to 255.76 and 273.25  $\mu\text{mol Trolox/g}$  sample, respectively, in CA-LF-Glc and CA-LF-PD ternary conjugates, indicating the glycosylation was an effective way to improve the antioxidant activity of the CA-LF conjugate. Moreover, the ternary conjugates were employed to encapsulate  $\beta$ -carotene as a model biologically active macromolecule, and they could enhance the physicochemical stability of  $\beta$ -carotene emulsions. This work presented a simple and general approach to the preparation of polyphenol-protein-polysaccharide conjugates that could be potentially employed as food-grade biomacromolecules in the food and pharmaceutical industries.

### Introduction

Proteins are widely utilized to enhance functional properties of food products, such as emulsification, gelling and foaming attributes.<sup>1</sup> However, the applications of food proteins are still limited, because they are generally unstable against heating, organic solvents and proteolytic attack.<sup>2</sup> If proteins can be transformed into stable forms, their applications will be prominently broadened in food industry.

Various protein modification technologies were extensively investigated, there were considerable evidences to suggest that covalent bonding of proteins with polysaccharides and/or polyphenol is an effective approach to overcome their instability under the unfavourable conditions and even induce a beneficial synergistic effect on the functional properties of the proteins.<sup>1-3</sup> Besides, conjugated proteins can be applied in the encapsulation and delivery system to provide an effective protection for bioactive compounds against thermo- or photodegradation and maximize the delivery efficiency.<sup>4-5</sup>

In recent years, the conjugation of proteins with

polysaccharides through spontaneous Maillard reaction has attracted significant attention. Maillard reaction is a promising method because it can alter the functionality of proteins without the presence of chemical reagents.<sup>1,6</sup> In the Maillard reaction, a protein and polysaccharide are linked through a covalent bond between the amino group of the protein, especially the  $\epsilon$ -amino group of lysine residues and the terminal reducing group of the carbonyl of the polysaccharide.<sup>1,7</sup> The formation of protein-polysaccharide conjugates by controlled dry heating seems to be the most effective method for the production of emulsifiers for food products.<sup>2,8</sup> Maillard reaction significantly increases food protein solubility, heat stability, emulsifying property, foaming property, antioxidant activity and antimicrobial property.<sup>1,9-11</sup> On the other hand, the conjugates formed by glycosylation also have potential applications in controlled release systems and nanoencapsulation.<sup>12-13</sup> Maillard-type protein-polysaccharide conjugates, which were natural, non-toxic and have improved functional properties, could be predictable to have extensive potential for application in the food and health industries.<sup>14</sup>

Phenolic compounds represent the largest group of secondary plant metabolites and are important food components with a large range of structures and functions.<sup>15</sup> Naturally occurring polyphenols are known to have numerous biological activities, in particular, they have recently received attention as antioxidants. Conjugating antioxidant molecules with protein forms new functionalized materials combined the properties of

<sup>a</sup> Beijing Laboratory for Food Quality and Safety, College of Food Science & Nutritional Engineering, China Agricultural University, 100083, China.

\*Corresponding author.  
Tel.: + 86-10-62737034; Fax: + 86-10-62737986  
E-mail: gyxcau@126.com

both molecules. In recent investigations it has been shown that the binding phenolic compounds to proteins leads to significant improvement in physicochemical properties and activities of proteins.<sup>15-16</sup> Phenolic compounds can covalently react with proteins in the form of a phenolic radical or quinone via enzymatic or non-enzymatic oxidation.<sup>17-19</sup> The non-enzymatic oxidation method has been applied extensively, and the results showed that phenolic oxidation products generated under alkaline condition could react with amino groups, thiol groups and tryptophan residues of the protein<sup>20</sup>. As a consequence, the modification induced the cross-linking of proteins and phenolic compounds and altered the physicochemical properties of proteins, such as the solubility, surface hydrophobicity, and emulsification, in addition, the covalent conjugation delivered proteins with enhanced antioxidant activity.<sup>21-22</sup>

However, to the best of our knowledge, there is no information so far concerning the characteristics of the polyphenol-protein-carbohydrate covalent complex. Based on the studies mentioned above, the ternary conjugation of protein, carbohydrate and polyphenol might be an attractive method to develop new food grade materials with better physicochemical properties by drawing advantages of the three components. In addition, the covalent reaction between carbohydrate and protein-polyphenol conjugate might be an encouraging way for the functionality modification of the biological macromolecule.

This work reports a rapid and eco-friendly procedure for the covalent complexing of polyphenol-protein molecules and glucose (Glc) /polydextrose (PD) by controlling pH and dry-heating process. Lactoferrin (LF), a mammalian cationic iron-binding glycoprotein belonging to the transferrin family, is raising great interest in food and medicinal researches owing to its health benefits.<sup>23-24</sup> Because of its biodegradability and biocompatibility in physiological environment, LF was chosen as a polymer backbone to be functionalized with chlorogenic acid (CA) and Glc/PD to obtain new biomacromolecules. The objective of this study is to (i) create and characterize ternary conjugates obtained via Maillard reaction between CA-LF conjugate and Glc as well as PD, respectively; (ii) evaluate the thermal stability and antioxidative properties of the conjugates compared to the native protein; (iii) apply the ternary conjugates to encapsulate  $\beta$ -carotene and evaluate the influence of processing and storage conditions on the physicochemical stability of  $\beta$ -carotene emulsions.

## Experimental

### Materials

Lactoferrin (LF) was obtained from Hilmar Ingredients (Hilmar, Calif., USA), the product contained 1.2% moisture, 0.3% ash and 99% protein, of which 96.1% was LF. Chlorogenic acid (CA, purity  $\geq 99\%$ ) was purchased from BSZH Science Company (Beijing, China). Glucose (Glc, purity  $\geq 99.0\%$ ) was purchased from Beijing Chemical Reagent (Beijing, China). Polydextrose (PD, type III, E12003) was supplied by Henan Tailijie Bioceth Co., Ltd. (Henan, China). Trolox (6-hydroxy-2, 5, 7, 8-tetramethylchroman-2-carboxylic

acid) was obtained from Sigma-Aldrich Chemie GmbH (Steinheim, Germany).  $\beta$ -Carotene suspension (30% by mass  $\beta$ -carotene in sunflower oil) was supplied by Xinchang Pharmaceutical Co., Ltd. (Zhejiang, China). Medium-chain triglyceride (MCT) oil was provided by Lonza Inc. (Allendale, NJ, USA). Standard  $\beta$ -carotene (purity  $>95\%$ ) was purchased from Sigma-Aldrich (St. Louis, Missouri, USA). Dialysis bag (molecular weight cut-off 12-14 kDa) was provided by Biodee Biotechnology Co., Ltd (Beijing, China). All other chemicals were of analytical grade, unless otherwise stated.

### Synthesis of CA-LF Conjugate

The CA-LF conjugate was synthesized according to the method of Rawel et al.<sup>25</sup> with slight modification. Briefly, 1.0 g LF was dissolved in 50 mL of distilled water and stirred overnight to ensure complete dispersion and dissolution, and then the pH value of the protein solution was adjusted to 9.0 with 0.1 M NaOH. To prepare CA-LF conjugate, 0.25 g CA was dissolved in 50 mL of distilled water and the pH was adjusted to 9.0. Then the protein solution was mixed with the CA solution under continuous stirring (120 rpm). To prevent microbial growth during sample preparation, sodium azide (0.02%, w/w) was added. After 24 h reaction process under continuous stirring at room temperature with free exposure to air, the samples were dialyzed for 48 h against water to remove free CA. Thereafter, the resulting solution was frozen and dried with Alpha 1-2 D Plus freeze-drying apparatus (Marin Christ, Germany) to obtain porous solids.

### Synthesis of CA-LF-Glc/PD Conjugates

LF, CA-LF conjugate and Glc/PD were respectively dissolved in distilled water at a concentration of 20 mg/mL and stirred overnight at 25 °C. Then CA-LF conjugate solution was mixed with Glc and PD solutions (1:1, w/w), respectively. Each sample was adjusted to pH 7.0 and then frozen-dried. The resultant powders were incubated at 60 °C/79% relative humidity (RH) in the presence of saturated KBr solution, for a period of 24 hours.<sup>26</sup> Unheated LF, CA-LF conjugate and mixtures of CA-LF conjugate and Glc/PD were prepared under the same condition, and served as controls.

### Measurement of UV Absorbance and Browning Extent

The UV-Vis analysis of the samples was performed using a spectrophotometer (UV-1800, Shimadzu, Kyoto, Japan). Samples were dissolved with distilled water (pH7.0) to a final concentration of 0.25 mg/mL and the sample was scanned with the wavelength ranging from 200 nm to 450 nm. The UV absorbance and browning extent of the samples were measured according to the method of Ajandouz et al.<sup>27</sup> The solutions of different samples were appropriately diluted and the absorbance was measured at 294 and 420 nm with distilled water as blank references, respectively.

### Analysis for the Degree of Graft

Degree of graft (DG) was indirectly determined from analysis of contents of free amino groups in the samples, following the ortho-phthaldialdehyde (OPA) method<sup>28</sup> with minor

modification. The OPA reagent was prepared freshly before used by mixing the following reagents: 40 mg of OPA (dissolved in 1 mL of methanol), 25 mL of 0.1 M sodium borate buffer (pH 9.85), 100  $\mu$ L of  $\beta$ -mercaptoethanol, and 2.5 mL of 20% (w/v) sodium dodecyl sulfate in deionized water. The mixture was diluted to 50 mL with deionized water. Then 4 mL of OPA reagent and 200  $\mu$ L of protein solution (4 mg/mL) were mixed thoroughly and then reacted in a 35 °C water bath for 2 min. After that, the absorbance at 340 nm was measured using a double beam spectrophotometer. The content of free amino groups was calculated by using the calibration curve of L-leucine as a standard.

Degree of graft (DG) of ternary conjugates was calculated from the loss in free amino groups compared to the mixture of CA-LF conjugate and Glc/PD as follows:

$$DG = (C_0 - C_1) / C_0 \times 100\%$$

Where  $C_0$  is the content of free amino groups of the mixture of CA-LF conjugate and Glc/PD,  $C_1$  is the content of free amino groups of the conjugates.

#### Matrix-Assisted Laser Desorption/Ionization Time-of-Flight Mass Spectrometry (MALDI-TOF-MS) Analysis

MALDI-TOF-MS measurements were performed on Autoflex-II TOF/TOF mass spectrometer (Bruker Daltonics, Billerica, MA, USA). Sinapinic acid was selected as the matrix and dissolved to saturation in a 1:1 mixture of 0.1% trifluoroacetic acid (TFA) and acetonitrile (50%, v/v). Briefly, 1 mg of the samples was dissolved in 1 mL of distilled H<sub>2</sub>O, then 0.5  $\mu$ L of these solutions was brought on to the target and covered with 0.5  $\mu$ L matrix. After crystallization by air-drying, the samples were analysed by MALDI-TOF-MS. The mass spectra were recorded in the reflector mode with an acceleration voltage of 20 kV and an effective flight path of 200 cm, and external calibration was obtained using bovine serum albumin.

#### Fourier Transform Infrared (FT-IR) Spectroscopy

The infrared spectra of the samples were obtained with the potassium bromide pellet method. The dried samples were ground into powders, pressed into pellets and measured by a Spectrum 100 Fourier transform spectrophotometer (Perkin-Elmer, UK) in 400–4000  $\text{cm}^{-1}$  range, at a resolution of 4  $\text{cm}^{-1}$ . KBr was used as a reference. For each measurement, 11 scans were taken. The data were analyzed using Origin 8.0 (OriginLab, Northampton, USA).

#### Circular Dichroism Spectra

Far-UV Circular dichroism spectra of the samples were recorded in the range 190–250 nm with 0.1 mg/mL sample by a Chirascan spectrometer (Applied Photophysics Ltd, UK) using a quartz cylindrical cell in 1 mm path length. Ellipticity was recorded at a speed of 100 nm/min, 0.2 nm resolution, 20 accumulations and 2.0 nm bandwidth. The collected data were analyzed using Dichroweb (Circular Dichroism Website <http://dichroweb.cryst.bbk.ac.uk>).<sup>29–30</sup>

#### Fluorescence Spectroscopy

Fluorescence steady state measurements were performed on a fluorescence spectrophotometer (Varian Instruments, Walnut Creek, CA, USA). Scanning parameters for all measurements were optimized with slit width 20 nm for excitation and 10 nm for emission. The concentration of the samples was 1 mg/mL. The excitation wavelength was set at 295 nm to selectively excite the tryptophan residues and the emission was collected between 320 and 380 nm.

#### Differential Scanning Calorimetry (DSC) Measurement

Calorimetric analyses were performed using a DSC-60 thermal analysis system (Shimadzu, Tokyo, Japan). In a standard procedure, about 5.0 mg of samples was placed inside an aluminum pan and sealed tightly by a perforated aluminum lid, heated from 30 to 120 °C at a constant rate of 10 °C/min with a constant purging of dry nitrogen at a rate of 30 mL/min. An empty aluminum pan was used as a reference. The peak temperature of denaturation was computed using the universal analysis software from each thermal curve.

#### Atomic Force Microscopy (AFM) Measurements.

AFM measurements of native LF, CA-LF conjugate and CA-LF-Glc/PD ternary conjugates/mixtures were performed by using a Nanoscope IIIa system (Digital Instruments, Veeco, Santa Barbara, California, USA) operating in tapping mode. Samples were diluted to a total protein concentration of 10 mg/L using deionized water, and aliquots (2  $\mu$ L) of the diluted sample were placed onto a freshly cleaved mica sheet that was fixed on an iron disk (Bruker Corp., Santa Barbara, California, USA). After air-drying for more than 2 h, AFM images were collected at a scanning rate of 1.0 Hz under ambient condition. Image analysis was conducted by using Digital Nanoscope software (version 5.30r3, Digital Instruments, Veeco, Santa Barbara, California, USA). For each experiment, at least five different areas were randomly chosen for imaging. The height and phase images were simultaneously recorded during AFM imaging.

#### Antioxidant Activities

**ABTS<sup>•+</sup> scavenging activity** The ABTS<sup>•+</sup> scavenging activity was evaluated according to Siddhuraju et al.<sup>31</sup> A stock solution of ABTS<sup>•+</sup> (7 mM) was prepared by diluting 10 mg of ABTS with 2.6 mL of potassium persulfate solution (2.45 mM). Then the mixture was kept in the dark for 12–16 h at room temperature before used. Thereafter, the ABTS working solution was diluted with distilled water to an absorbance of 0.70±0.02 at 734 nm. Then 1 mL of the sample (0.5 mg/mL) and 3 mL of ABTS solution were mixed, incubated at room temperature for 1 h, and the absorbance at 734 nm was then measured using a spectrophotometer. The scavenging activities of samples were measured as the decrease of the absorbance and expressed as percent scavenging of ABTS<sup>•+</sup>.

**Reducing Power** The ability of samples to reduce iron (III) was determined according to Yildirim et al.<sup>32</sup> Specifically, 1 mL of the sample was mixed with 2.5 mL of 0.2 M sodium phosphate buffer (pH 6.6), and the reaction was initiated by addition of 1% (w/v) potassium ferricyanide. The mixtures were incubated

at 50 °C for 20 min. After that, 2.5 mL of 10% (w/v) trichloroacetic acid was added and the mixture was centrifuged at 3000×g for 10 min. Finally, 2.5 mL of the supernatant was mixed with 0.5 mL of distilled water and 0.1 mL of FeCl<sub>3</sub> (0.1%, w/v), followed by the measurement of absorbance at 700 nm using a spectrophotometer. A higher absorbance indicates higher reducing power. The reducing power was calculated on basis of the Trolox calibration curve, which was carried out by the method mentioned above, and expressed as μmol Trolox equivalents per g sample.

#### Preparation of β-Carotene Emulsions

LF, CA-LF conjugate, and CA-LF-Glc/PD mixtures and conjugates were first dispersed in distilled water at a protein concentration of 0.7 wt%, separately. And then the solutions were stirred overnight to ensure complete dispersion and dissolution, while sodium azide (0.02% w/v) was added to prevent microbial growth. β-Carotene emulsions were prepared according to a previous study<sup>33</sup> with slight modification. Briefly, β-carotene (0.1 wt% in the final emulsion) was first dissolved in medium chain triacylglycerol (MCT) oil (5 wt% in the final emulsion) at 140 °C for 30 seconds, and then mixed with different aqueous phase by using an Ultra-Turrax (Model T25, IKA-Works, Inc., Cincinnati, Ohio, USA) at a speed of 10000 rpm for 10 min to form coarse emulsions, which were further homogenized using a Niro-Soavi Panda two-stage valve homogenizer (Parma, Italy) for three cycles at 60 MPa. The final emulsions were immediately cooled down to 25 °C and sampled to measure the particle characteristics. The residual emulsions were transferred into screw-capped brown bottles and stored at 4 °C in the dark.

#### Measurement of Droplet Size and ζ-potential

Particle size and size distribution were determined by dynamic light scattering (DLS) using a Zetasizer Nano-ZS90 (Malvern Instruments, Worcestershire, UK) at a fixed angle of 90°. Conjugated nanoparticles were determined at a total protein concentration of 1mg/mL, and β-carotene emulsions were diluted (1:500) with deionized water prior to analysis to minimize multiple scattering effects. The ζ-potential was determined by measuring the direction and velocity of droplet movement in a well-defined electric field. The data were collected from at least 10 sequential reading per sample after 60s of equilibration, and the data were calculated by the instrument using the Smoluchowski model. All measurements were performed in triplicate.

#### Measurement of Physicochemical Stability of β-Carotene Emulsions

**Thermal stability** The β-carotene emulsions were incubated at boiling water (100 °C) for 5 min, and then cooled down and stored for 1 week. The sizes were measured to evaluate the stability of β-carotene emulsions.

**Freeze-thaw stability** The β-carotene emulsions (5 mL) were transferred into cryogenic test tubes, which were incubated in a -18 °C freezer for 20 hours and then thawed by placing them in

a water bath at 30 °C for 2 hours.<sup>34</sup> The sizes were evaluated before and after the freeze-thaw treatments.

**pH stability** The pH of β-carotene emulsions was adjusted to 3.0 using 0.1 M HCl or NaOH, and then the sizes were measured to evaluate the stability of β-carotene emulsions.

**NaCl stability** NaCl was dissolved in deionized water to prepare 0.8 mol/L NaCl solution. The emulsions were mixed with the same volume of NaCl solution. The mixtures were shaken fully and placed at 25 °C for 6 h and the droplet sizes were determined.

**Stability of β-carotene in emulsions** Emulsion samples were diluted with deionized water (1:4) and then transferred into screw-capped brown bottles flushed with nitrogen. Each emulsion sample was stored at 25 °C and 37 °C respectively in dark immediately after the dilution. β-Carotene content in the emulsion was determined according to Yuan et al.<sup>35</sup> during the storage.

#### Statistical Analysis

All experiments were performed in triplicate and the results were expressed as mean value ± standard deviation in this study. Data were analyzed by the software package SPSS 18.0 (SPSS Inc., Chicago, USA). Statistical differences were determined by One-way analysis of variance (ANOVA) with Duncan's post hoc test, and differences were considered to be significant with  $p < 0.05$ .

## Results and Discussion

### Physicochemical Properties of Ternary Conjugates

**Changes in UV-vis absorbance and browning intensity** UV-vis spectra of LF, CA-LF, and CA-LF-Glc/PD mixtures and conjugates were compared (Fig. 1a). CA has an absorbance maximum at 324 nm (data not shown), which was absent in the LF control, but present as a shoulder in the spectra of CA-LF conjugate. It can be observed that the ternary conjugates and mixtures showed different absorptions in the UV-vis spectra, although they had similar shapes. The absorbance of the ternary conjugates increased significantly compared to the mixtures, and the peak of the ternary conjugates had a maximum absorbance that appeared in the range 260–300 nm, which is characteristic of melanoidins.<sup>36</sup> These results indicated that the glycosylation of CA-LF conjugate could enhance its absorption in the ultraviolet region.

The colour of conjugated products was a direct and easy indication of Maillard reaction progress. Ultraviolet absorbance ( $A_{294}$  nm) and brown colour ( $A_{420}$  nm) are typical indicators of colourless intermediate compounds and final browning compounds, respectively.<sup>27</sup> The changes of  $A_{294}$  and  $A_{420}$  of ternary conjugates were shown in Fig. 1b. It could be found that both  $A_{294}$  and  $A_{420}$  of LF significantly increased after its conjugation with CA, this was mainly owing to the formation of protein-polyphenol covalent complexes. Sabir et al.<sup>37</sup> demonstrated that under neutral and alkaline conditions, sunflower protein solutions developed dark green and brown colours as a result of the covalent bonding with oxidation

products of CA. Meanwhile, compared with CA-LF-Glc/PD mixture, CA-LF-Glc/PD ternary conjugates showed the increased absorbance values of  $A_{294}$  and  $A_{420}$ , which were characteristic indexes of the formation of intermediate compounds of the Maillard reaction. In addition, the  $A_{294}/A_{420}$  absorbance ratio was indicative of the polymerization extent.<sup>27</sup> Via calculating from the data in Fig. 1b, CA-LF-Glc conjugate exhibited the higher level of polymerization than CA-LF-PD conjugate. Therefore, these results analyses corroborated the occurrence of the Maillard reaction and confirmed that brown polymers were generated at the advanced stage.

**Changes of Free Amino Groups' Content** When evaluating the formation of protein-polyphenol conjugates, the estimation of modified amino acids is a critical method to analyze the extent of phenolic compound bound,<sup>15</sup> which is also commonly used to determine the progress of Maillard reaction, since it occurs by covalent attachment of carbonyl group in reducing sugars with free amino groups in proteins to form Schiff base.<sup>38</sup> In this study, the primary amino group availability in the protein was investigated using the OPA method. The amount of free amino groups in LF was reduced by 40.32% after the covalent binding between LF and CA, as the analysis was conducted in presence of 1% SDS (which destroys non-covalent protein interactions), we can suppose that the derivatization occurred through covalent binding. With dry-heating treatment for 24 h, the content of free amino groups in the CA-LF-Glc and CA-LF-PD conjugates was significantly reduced. As shown in Fig. 1c, the DG was 40.5% for CA-LF-Glc conjugate, and 11.72% for CA-LF-PD conjugate, indicating Maillard reaction between CA-LF conjugate and Glc occurred to a higher extent. These results interpreted that the Maillard reaction took place differently between CA-LF conjugate and two types of carbohydrates, the largely incomplete reaction with PD might be attributed to the steric hindrance. Because PD is an oligomer of Glc,<sup>39</sup> not all lysines are accessible, this steric hindrance was increased with the conjugation of PD molecules to LF.

**Fig. 1**

#### Confirmation of CA-LF-Glc/PD Conjugates by MALDI-TOF-MS

MALDI-TOF MS is a high sensitivity technique that provides detailed structural information about the individual molecules contained in a polymer sample, it can potentially provide quantitative information required for determination of the average molecular mass and molecular mass distribution of a polymer.<sup>40</sup> Analysis of molecular masses of native LF, control LF (heat-treated LF), native CA-LF conjugate, control CA-LF conjugate (heat-treated CA-LF conjugate) and CA-LF-Glc/PD ternary conjugates by MALDI-TOF MS was conducted to confirm the occurrence of the reaction described above and to investigate the extent of the glycosylation. The mass spectra of the samples were presented in Fig. 2. The mass of native LF showed a peak at 84011.15, which was in agreement with its sequence. The spectrum profile of the control LF was very similar to that of the native LF, suggesting that dry heating did not cause any change in the molecular weight profile of LF. In case of native CA-LF conjugate, there was an increase in the

molecular weight of 1058 corresponding to 3 CA molecules bound to 1 LF molecule. Moreover, it could be clearly observed from Fig. 2 that the dry heating induced substantial aggregation in the CA-LF conjugates, probably as a consequence of the covalent bonding of CA-LF conjugate with the exposed amino acids. Furthermore, the reaction of CA-LF conjugate with Glc and PD resulted in the higher-molecular mass species, which might have been caused by the introduction of Glc/PD to the CA-LF conjugate and the subsequent increase in the molecular mass. It was interesting to note that the mass of CA-LF-Glc conjugate was higher than that of CA-LF-PD conjugate, though Glc is a small molecule compared with PD, implying that the greater extent of reactivity between CA-LF conjugate and Glc. This phenomenon was attributed to the difference in structures of Glc and PD. PD was initially produced by vacuum-melt condensation of Glc, which is a highly branched indigestible Glc polymer with an average degree of polymerisation of ten or twelve Glc molecules.<sup>41-42</sup> Thus, at the same mass ratio between protein and the carbohydrates in the Maillard reaction, Glc has higher reaction activity than PD for more C-terminals molecules. In addition, it was generally admitted that the sugar reactivity was directly to the proportion of the active carbonyl species in the solution, Glc was characterized by a more accessible carbonyl function, which was probably another explanation why it was more reactive.<sup>43</sup>

**Fig. 2**

Generally, polyphenols can be oxidized in an alkaline solution to its corresponding quinone, and then being a reactive electrophilic intermediate, could readily undergo attack by nucleophiles such as lysine, cysteine and tryptophan moieties in a protein chain, leading to the formation of cross-linked protein polymers<sup>20</sup>. According to Folin-Ciocalteu method (data not shown), the amount of CA covalently bound to LF was 27.26mg g<sup>-1</sup> CA-LF conjugates, with a reaction percentage yield of 13.63%.

In this study, the available amino group of the CA-LF conjugate could then react with the reducing end of the carbohydrate. The proposed scheme of the formation of ternary conjugates was shown in Fig. 3, CA was readily oxidized to its respective quinone, the CA quinone may form a dimer or polymer in a side reaction, and then reacted with amino or sulfhydryl side chains of LF, to generate covalent C-N or C-S bonds with the phenolic ring, with restructuring of hydroquinone. The latter might be reoxidized and bind a second protein, therefore it comes to cross-links of protein molecules, resulting in the polymerization. The available amine groups of the resulting polymer can react with the carbonyl group of Glc or PD, to form an N-glycosylamine with the release of one water molecule.<sup>44</sup> The N-glycosylamine undergoes an irreversible rearrangement generating the Amadori product, which may be altered by oxidation, fragmentation, dehydration, and free radical reactions, resulting in the formation of CA-LF-Glc/PD conjugates.

**Fig. 3**

#### Structural Characterization of CA-LF-Glc/PD Ternary Conjugates

**FTIR analysis** The chemical structures of the ternary conjugates were characterized by FTIR measurement. Figure 4 showed the infrared spectral changes of LF, CA-LF conjugate and CA-LF-Glc/PD conjugates. FTIR profiles revealed that some pronounced differences among native LF, CA and CA-LF conjugate (Fig. 4a), and distinguished CA-LF-Glc/PD conjugates from the CA-LF-Glc/PD mixtures (Fig. 4b). CA has three characteristic peaks around 3350, 3467 and 3618  $\text{cm}^{-1}$ , probably due to the vibration of the O-H linkage of phenolic hydroxyl groups, and two large peaks around 1686 and 1639  $\text{cm}^{-1}$ , probably due to the carbonyl stretching of CA, while those peaks were not found in CA-LF conjugate at all. In the FTIR measurement of LF, the assignments of representative peaks have been already clarified, the characteristic absorption bands at around 3300  $\text{cm}^{-1}$ , 1651  $\text{cm}^{-1}$ , and 1533  $\text{cm}^{-1}$  were assigned to amide A (representative of N-H stretching coupled with hydrogen bonding), amide I (representative of stretching/hydrogen bonding coupled with COO-) and amide II (representative of C-N stretching coupled with NH bending modes), respectively.<sup>18</sup> When CA was bound to LF, we could find that there was more or less spectral shifting for the protein amide A and amide I band, suggesting that the interaction of CA with skeletal N-H, C-O or COO- group of LF molecules most likely caused the conformational change of the protein. In addition, it could be found that there was a noticeable change in amide II, attributed to skeletal C-N and C=C vibrations, which might be due to the oxidation of CA and formation of more complicated dimeric-structures in the covalent reaction process.<sup>45</sup>

It might be predictable that Maillard reaction between CA-LF conjugate and carbohydrates could lead to loss of functional groups including  $\text{NH}_2$ , especially from lysine, while their amount associated with Maillard products such as the Amadori compound (C=O) and Schiff base (C=N) may be increased, these chemical changes would lead to some alterations in the FTIR spectrum.<sup>46</sup> For carbohydrates, a series of overlapping peaks located in the region of 1180–953  $\text{cm}^{-1}$  resulted from vibration modes such as the stretching of C-C and C-O and the bending mode of C-H bonds, these absorptions are weak in the spectra of most proteins.<sup>47</sup> Fig. 4b showed the infrared spectral changes of CA-LF-Glc/PD mixtures/conjugates. Compared with the CA-LF-Glc/PD mixtures, there were obvious red shifts at amide A in the spectra of CA-LF-Glc/PD conjugates (especially for CA-LF-PD conjugate with 90 nm), the absorption band located at 3300–3400  $\text{cm}^{-1}$  could be attributed to the  $-\text{NH}_2$  and  $-\text{OH}$  stretch vibration,<sup>48</sup> suggesting the modification of LF amino groups in these regions. Regions of 1651 and 1533  $\text{cm}^{-1}$ , denoted as C=O and C-N stretching from amide I and II, were modified by the Maillard reaction, because the intensity of CA-LF-Glc/PD conjugates decreased compared to CA-LF-Glc/PD mixtures. In addition, there were some variations in the peaks of CA-LF-Glc/PD conjugates at around 1445–1448  $\text{cm}^{-1}$  attributes to  $\text{CH}_2$  stretching, and 1050–950  $\text{cm}^{-1}$  corresponds to side-chain vibrations from the protein regions,<sup>49</sup> indicating the alteration of protein structure.

**Fig. 4**

**Second Structure Analysis** Circular dichroism spectra are remarkably sensitive to the secondary structure of proteins.<sup>50</sup> In this study, Far-UV circular dichroism spectra were used to characterize the secondary structures of LF in the mixtures and conjugates, the estimated secondary structures were shown in Table 1. As indicated in Fig. 5a, the far-UV of the native LF displayed a negative minimum at 209 and a maximum at 190–195 nm, which is typical of  $\alpha$  class protein. The conjugation of LF with CA caused a decrease in band intensity at all wavelengths in the far-UV spectrum, without any significant shift of the peaks. However, the change of the intensity resulted from a decrease in  $\alpha$ -helix and an increase in unordered structure (Table 1), similar to that observed by Rawel et al.,<sup>25</sup> who revealed that covalent interaction of CA with bovine serum albumin cause a decrease in  $\alpha$ -helix structure, with a parallel increase in unordered structure. It was reported that covalent binding of polyphenols with different protein chains could result in full or partial unfolding or denaturation of the protein chains by altering their secondary and tertiary structures,<sup>51</sup> hydrophobic interactions between polyphenol and pralines residues,<sup>25</sup> electrostatic effects and hydrogen bonds<sup>51</sup> could influence protein  $\alpha$ -helical intermediate formation.

In the case of Maillard reaction products, compared with CA-LF-Glc/PD mixtures, the CA-LF-Glc/PD conjugates extremely lost the  $\alpha$ -helix structure with a concomitant increase in turns and unordered proportions. These results indicated that the secondary structure of CA-LF conjugate might be changed by Maillard reaction procedure. Some researchers<sup>52–53</sup> reported that the Maillard reactions between proteins and carbohydrates could affect the secondary structure of proteins, which was not only due to the interaction of biopolymers but also to the heat denaturation of proteins during the treatment. In this study, when Glc/PD were added to CA-LF conjugate, the hydrogen bonds could be formed, which probably had an intermolecular interaction among the neighbouring proteins and led to the increased amount of  $\alpha$ -helix and reduced the amount of intermolecular unordered structure. After the CA-LF-Glc/PD mixtures was heated, the hydrogen bonds between Glc/PD and CA-LF conjugate were reduced, the conjugation of CA-LF and Glc/PD could possibly impair the intermolecular interaction, which would finally lead to a reduction of  $\alpha$ -helix.<sup>54</sup>

**Table 1**

**Emission Fluorescence Spectroscopy Analysis** LF was considered to have intrinsic fluorescence because of tryptophan and tyrosine residues. At 295 nm wavelength, tryptophan residue was excited and the quenching could take place when the quencher was sufficiently close to it.<sup>55</sup> A possibility of the reaction between CA and tryptophan was also studied by Wang et al.<sup>33</sup> The fluorescence emission spectra of LF, CA-LF conjugate and CA-LF-Glc/PD ternary conjugates were shown in Fig. 5b. When the excitation was at 295 nm, LF exhibited a fluorescence maximum emission ( $\lambda_{\text{max}}$ ) at 336 nm. Pronounced quenching effects were observed in case of CA-LF conjugate, which presumably involved a Forster type fluorescence resonance energy transfer (FRET). In addition, both the CA-LF-Glc/PD mixtures and conjugates showed a decreased

maximum emission and marked red shifts of the  $\lambda_{\text{max}}$  relative to the CA-LF conjugate. These findings proved that tryptophan residues in the ternary mixtures and conjugates were largely surrounded to a hydrophobic environment and the protein might have more compact tertiary conformations compared to native LF and CA-LF conjugate.<sup>53</sup> It is believed that the conjugate layer of carbohydrates could efficiently reduce the fluorescence intensity,<sup>56</sup> the fluorescence intensity of CA-LF-Glc conjugate was remarkably lower than that of CA-LF-Glc mixture, which implied the former had a thicker layer and formed a shielding effect.<sup>28</sup>

### Fig. 5

**DSC Analysis** Thermal characterization of native LF, CA-LF conjugates and CA-LF-Glc/PD mixtures/conjugates was also performed by recording of DSC thermograms, the characteristic parameters were summarized in Table 2. Native LF was observed to generate two endothermic peaks at 68.4 and 89.1 °C, which was corresponded to the two denaturation temperatures (*T<sub>d</sub>*). These peaks were attributed to the difference in the heat sensitivity of the two lobes of LF, since the C lobe seemed more compact than the N lobe in the iron-saturated protein.<sup>57</sup> However, CA-LF conjugate showed one endothermic peak, at a higher temperature than native LF (compared with the first *T<sub>d</sub>*), indicating the modification of CA enhanced thermal stability of LF. In addition, the covalently modified LF required less energy to unfold, since the  $\Delta H$  was decreased when compared with native LF. These results were in agreement with the findings reported by Liu et al.,<sup>18</sup> who demonstrated that the modification with CA by radical polymerization could increase the denaturation temperature of LF.

In general, the glycation could lead to an increase of *T<sub>d</sub>* and a decrease of  $\Delta H$ , indicating the improved thermal stability or tertiary conformational stability of proteins.<sup>7</sup> In this study, *T<sub>d</sub>* values of CA-LF-Glc/PD mixtures/conjugates were significantly higher than that of native LF ( $p < 0.05$ ), and CA-LF-Glc/PD conjugates have higher values of *T<sub>d</sub>* than that of CA-LF conjugate. Thus, the thermal stability of CA-LF conjugate was remarkably improved by Maillard-type conjugation. Furthermore, the  $\Delta H$  values of CA-LF-Glc/PD conjugates were decreased compared with CA-LF-Glc/PD mixtures, a lower  $\Delta H$  value suggested that less energy was required for the denaturation, which might be attributed to the partial denaturation of CA-LF conjugate in the Maillard reaction. These findings indicated a protective effect of the glycation on the thermal denaturation of LF.

### Table 2

**Particle Size,  $\zeta$ -Potential and Morphology Analysis** DLS has been proved to be an effective technique for analyzing the size and size distribution of polymers, proteins and nanoparticles in suspension, based on the Brownian motion of spherical particles.<sup>58</sup> AFM observation and DLS analysis were performed in order to determine the particles morphology and dimensions of the conjugates (Fig. 6). Native LF, a globular protein, is a small globule of non-uniform size (6.5 nm), with an average  $\zeta$ -potential of about +25.7 mV. For CA-LF conjugate, the AFM

image showed regular globular shape with smooth surface, and the average diameter was about 10.10 nm, slightly bigger than that of native LF. However, the  $\zeta$ -potential of CA-LF conjugate was about -7.73 mV, this is because covalent modification of the protein with CA could change its isoelectric point (PI) to a lower pH value,<sup>25</sup> the CA-LF conjugate carried negative charge when the pH of the solution was higher than the PI, the absolute  $\zeta$ -potential value of CA-LF conjugate was smaller than that of LF, this phenomenon could be explained by the fact that CA conjugated to LF lowered the electrophoresis mobility. Meanwhile, the particles of the ternary mixtures were partial irregular in shape, with a mean size of  $13.47 \pm 0.28$  nm, resulting in a polydispersed distribution. Compared with CA-LF-Glc/PD mixtures, the ternary conjugates showed coarser structure and bigger particles size, the greater hydrodynamic size of the conjugate particles indicated the formation of higher molecular weight polymers. Besides, the conjugating reaction was not homogeneous, the spherical structure was almost disappeared in the ternary conjugates, and therefore, it suggested that the conjugates might have core-shell structure, the CA-LF conjugate molecules conjugating with Glc/PD located on the surface of the core, while those without conjugation located inside the core. It is important to note that the  $\zeta$ -potential values of the conjugates were different from those of the mixtures, CA-LF-Glc conjugate exhibited the highest  $\zeta$ -potential among the conjugates, indicating the best stability based on electrostatic repulsion.

### Fig. 6

#### Antioxidant Activities of the Conjugates

Some Maillard reaction products (MRPs) have been shown to contribute greatly to the shelf-life of heat-treated foods because of their antioxidant, antiallergenic, antimicrobial and cytotoxic properties, many studies were focused on the high antioxidant capacity of MRPs in model systems and foods such as beer, coffee and bakery products.<sup>59</sup> The ABTS<sup>•+</sup> scavenging activity and the reducing power of LF, CA, CA-LF conjugate and CA-LF-Glc/PD mixtures/conjugates were shown in Fig. 7a and 7b, respectively. It could be found that native LF showed little ABTS<sup>•+</sup> scavenging activity and reducing power, however, the CA-LF conjugate exhibited higher ( $p < 0.05$ ) antioxidant activity, with 2.73-fold ABTS<sup>•+</sup> radical scavenging activity and 1.86-fold reducing power of LF. These results indicated that the covalent incorporation of CA onto LF could strongly scavenge the radicals and formed more stable products, and finally terminated the radical chain reaction.

With regard to the antioxidant activity of chlorogenic acid, the ABTS<sup>•+</sup> scavenging activity was 84.41% and the reducing power was 205.72  $\mu\text{mol Trolox/g}$  CA-LF conjugate (an equivalent amount of free CA). As a consequence of the covalent binding between CA and LF, the ABTS<sup>•+</sup> scavenging activity of CA was significantly ( $p < 0.05$ ) decreased, which may be attributed to the polymerization mechanism in Fig. 3. In addition, the steric hindrance might be partly responsible for the loss of the antioxidative ability of the covalently bound phenolic compound.<sup>60</sup>



Compared with unheated CA-LF-Glc/PD mixtures, CA-LF-Glc/PD conjugates presented the enhanced antioxidant capacities. The ABTS<sup>•+</sup> scavenging activity and reducing power of MRPs derived from Glc and PD had no significant differences but were higher than those of the corresponding mixtures. It is supposed that the antioxidant effect was related to the development of intermediate reductone compounds, which were reported to break the radical chain by donation of a hydrogen atom, and were regarded as terminators of free radical chain reactions.<sup>61</sup> By comparing the reducing power and radical-scavenging activity of the ternary conjugates and those of CA-LF-Glc/PD mixtures, it could be found that the antioxidant activity of the protein was greatly improved by the modification of CA and Glc/PD. Therefore, CA-LF-Glc/PD ternary conjugates might be used as effective antioxidants to prevent lipid oxidation in food products.

**Fig. 7**

#### Stability of $\beta$ -Carotene Emulsions Stabilized by CA-LF-Glc/PD Conjugates under Different Processing Conditions

The purpose of these experiments was to investigate the emulsifying properties of CA-LF-Glc/PD conjugates and examine the effect of environmental stresses (thermal processing, freeze-thaw cycling, low pH and high ionic strength) on the sizes of  $\beta$ -carotene emulsions. The droplet sizes of original and heating emulsions were presented in Fig. 8a. Compared with the conjugates, the droplet size of original emulsions stabilized by the mixtures of CA-LF conjugate and Glc/PD was larger, which indicated that the non-covalent carbohydrate molecules tended to enhance droplet flocculation phenomena through depletion effects. After heating, the droplet sizes of the emulsions stabilized by CA-LF-Glc/PD conjugates were significantly smaller than those by the mixtures, CA-LF-Glc conjugate exhibited better stability than CA-LF-PD conjugate.

The influence of freeze-thaw cycling on droplet size of emulsions was shown in Fig. 8b. In comparison with the mixtures stabilized emulsions, CA-LF-Glc/PD conjugates stabilized emulsions had smaller size, demonstrating a better freeze-thaw stability, which might be attributed to the formation of a thick interfacial coating surrounding the oil droplets that resisted rupture during freezing and prevented the droplet aggregation.

Since acidic pH and high ionic strength are often found in food systems, the mean size of emulsions was measured at both acidic and high ionic strength environment to evaluate the potential applications of these conjugates in food industry. Fig. 8c showed the droplet sizes of emulsions at pH 3.0 and 6.0. The droplet sizes of CA-LF-Glc mixture/conjugate stabilized emulsions at pH 3.0 were similar to those of the initial emulsions (pH 6.0), in ternary conjugates-stabilized emulsions they were smaller than those in the mixtures at pH 3.0, which indicated that the conjugates were efficient in forming stable emulsions under acidic condition. Fig. 8d showed droplet sizes of emulsions containing electrolyte (400 mM NaCl). Due to the electrostatic screening and ion binding effects reduced the electrostatic repulsion between the oil droplets, the emulsions

stabilized by LF and the CA-LF conjugate were unstable to droplet aggregation in the presence of NaCl, but the CA-LF-Glc conjugate stabilized emulsion was stable against the aggregation, and average size of the emulsions stabilized by CA-LF-Glc/PD conjugates was significantly ( $p < 0.05$ ) smaller than those stabilized by CA-LF-Glc/PD mixtures, which interpreted clearly that the structure or thickness of interfacial membrane formed by Maillard-type conjugates were highly effective in stabilizing O/W emulsions. These results were in agreement with Zhu et al.,<sup>62</sup> who stated that covalent bonds produced between whey protein isolate (WPI) and dextran in Maillard-type conjugate was very stable against the change in pH, temperature, and ionic strength, and the emulsifying properties was improved over the native WPI due to thick steric barrier, increased oil droplet surface hydrophilicity by polysaccharide or adsorptive ability by the unfolded structure of protein, and decreased noncovalent interaction.

**Fig. 8**

#### Chemical Stability of $\beta$ -Carotene in Emulsions Stabilized by CA-LF-Glc/PD Conjugates under Storage Condition

Due to the highly unsaturated chemical structure,  $\beta$ -carotene is prone to degradation during processing and storage. Conjugating antioxidants (such as EGCG, CA) with a protein or polysaccharide as an emulsifier could be an effective way to retard  $\beta$ -carotene degradation in emulsions.<sup>33, 63</sup> The influence of CA-LF-Glc/PD conjugates on the chemical stability of  $\beta$ -carotene in emulsions was examined. Fig. 9 showed the degradation profile of  $\beta$ -carotene in emulsions stabilized with LF, CA-LF conjugate and CA-LF-Glc/PD mixtures/conjugates as a function of storage time.

**Fig. 9**

After the storage at 25 °C and 37 °C for a period of time, obvious loss of  $\beta$ -carotene was observed in emulsions stabilized by native LF and CA-LF-PD mixture, whereas the degradation of  $\beta$ -carotene in emulsions stabilized by CA-LF-PD conjugate was obviously retarded. After 3 weeks of the storage at 37 °C, the losses of  $\beta$ -carotene in the emulsions prepared with CA-LF-PD mixture and LF were 66.8% and 64.1%, respectively, but about 48.0 % for CA-LF-PD conjugate stabilized emulsion. These results were attributed to that the conjugate could form a thicker interfacial layer in emulsion droplets than the protein alone, which could also impact the diffusion of oxygen, free radicals, and pro-oxidants at oil-water interface. In addition, Maillard-type conjugates exhibited better antioxidant potential than the mixtures and the protein alone, which could also scavenge free radicals and consequently avoided the oxidation and degradation of  $\beta$ -carotene.<sup>63-64</sup>

## Conclusions

CA-LF-Glc/PD ternary conjugates were successfully prepared using a naturally occurring Maillard reaction between CA-modified LF and Glc as well as PD under mild condition. Formation of ternary conjugates was confirmed by MALDI-TOF-MS, FTIR spectroscopy, DSC and fluorescence analyses.

The covalent processes significantly altered the physicochemical and structural properties of LF and the conjugates were of high-antioxidative, heat-resistant and colloiddally stable properties. By applying the conjugates as emulsifiers, they were shown to be effective to enhance physicochemical stability of  $\beta$ -carotene emulsions under processing and storage conditions. This study demonstrates that CA-LF-Glc/PD conjugates are suitable biomacromolecules for the protection and delivery of bioactive compounds in food and pharmaceutical industries.

## Acknowledgements

We thank Dr. Yanxia Jia of Chinese Academy of Sciences for assistance in the AFM analysis. Financial support from the National Natural Science Foundation of China (No. 31371835) is gratefully acknowledged.

## Abbreviations

LF, lactoferrin; CA, chlorogenic acid; Glc, glucose; PD, polydextrose; CA-LF con, chlorogenic acid-lactoferrin conjugate; CA-LF-Glc con, chlorogenic acid-lactoferrin-glucose ternary conjugate; CA-LF-Glc mix, mixture of lactoferrin-chlorogenic acid conjugate and glucose; CA-LF-PD con, chlorogenic acid-lactoferrin-polydextrose ternary conjugate; CA-LF-PD mix, mixture of lactoferrin-chlorogenic acid conjugate and polydextrose; MALDI-TOF-MS, matrix-assisted laser desorption/ionization time-of-flight mass spectrometry; FTIR, Fourier transform infrared spectroscopy; DSC, differential scanning calorimetry; AFM, atomic force microscopy; DLS, dynamic light scattering; PI, isoelectric point; Td, denaturation temperatures. DG, degree of graft.

## Notes and references

- Oliver, C. M.; Melton, L. D.; Stanley, R. A. *Crit. Rev. Food Sci. Nutr.* 2006, **46**, 337-350.
- Kato, A. K. I. O. *Food Sci. Technol. Res.* 2002, **8**, 193-199.
- Jakobek, L. *Food Chem.* 2015, **175**, 556-567.
- Xu, D.; Wang, X.; Jiang, J.; Yuan, F.; Gao, Y. *Food Hydrocolloid.* 2012, **28**, 258-266.
- Zhou, H.; Sun, X.; Zhang, L.; Zhang, P.; Li, J.; Liu, Y. N. *Langmuir*, 2012, **28**, 14553-14561.
- Li, C.; Liu, F.; Gong, Y.; Wang, Y.; Xu, H.; Yuan, F.; Gao, Y. *LWT-Food Sci. Technol.* 2014, **57**(2), 612-617.
- Liu, J.; Ru, Q.; Ding, Y. *Food Res. Int.* 2012, **49**, 170-183.
- Einhorn-Stoll, U.; Ulbrich, M.; Sever, S.; Kunzek, H. *Food Hydrocolloid*, 2005, **19**, 329-340.
- Vhangani, L. N.; Van Wyk, J. *Food Chem.* 2013, **137**, 92-98.
- Liu, Q.; Kong, B.; Han, J.; Sun, C.; Li, P. *Food Structure*, 2014, **1**, 145-154.
- Wang, Y.; Liu, F.; Liang, C.; Yuan, F.; Gao, Y. *J. Sci. Food Agri.* 2014, **94**, 2986-2991.
- Deng, W.; Li, J.; Yao, P.; He, F.; Huang, C. *Macromol. Biosci.* 2010, **10**, 1224-1234.
- Markman, G.; Livney, Y. D. *Food Funct.* 2012, **3**, 262-270.
- Akhtar, M.; Dickinson, E. *Colloid. Surface. B.* 2003, **31**, 125-132.
- Rohn, S. *Food Res. Int.* 2014, **65**, 13-19.
- Ozidal, T.; Capanoglu, E.; Altay, F. *Food Res. Int.* 2013, **51**, 954-970.
- Prigent, S. V.; Voragen, A. G.; Visser, A. J.; van Koningsveld, G. A.; Gruppen, H. *J. Sci. Food Agri.* 2007, **87**, 2502-2510.
- Liu, F.; Sun, C.; Yang, W.; Yuan, F.; Gao, Y. *RSC Adv.* 2015, **5**, 15641-15651.
- Wei, Z.; Yang, W.; Fan, R.; Yuan, F.; Gao, Y. *Food Hydrocolloid*, 2015, **45**, 337-350.
- Kroll, J.; Rawel, H. M.; Rohn, S. *Food Sci. Technol. Res.* 2003, **9**, 205-218.
- Ali, M.; Homann, T.; Khalil, M.; Kruse, H. P.; Rawel, H. J. *J. Agric. Food Chem.* 2013, **61**, 6911-6920.
- Wang, X.; Zhang, J.; Lei, F.; Liang, C.; Yuan, F.; Gao, Y. *Food Chem.* 2014, **150**, 341-347.
- Ward, P. P.; Uribe-Luna, S.; Conneely, O. M. *Biochem. Cell Biol.* 2002, **80**, 95-102.
- Orsi, N. *Biometals*, 2004, **17**, 189-196.
- Rawel, H. M.; Rohn, S.; Kruse, H. P.; Kroll, J. *Food Chem.* 2002, **78**, 443-455.
- Moscovici, A. M.; Joubran, Y.; Briard-Bion, V.; Mackie, A.; Dupont, D.; Lesmes, U. *Food Funct.* 2014, **5**, 1898-1908.
- Ajandouz, E. H.; Tchiakpe, L. S.; Ore, F. D.; Benajiba, A.; Puigserver, A. *J. Food Sci.* 2001, **66**, 926-931.
- Vigo, M. S.; Malec, L. S.; Gomez, R. G.; Llosa, R. A. *Food Chem.* 1992, **44**(5), 363-365.
- Lobley, A.; Whitmore, L.; Wallace, B. A. *Bioinformatics*, 2002, **18**, 211-212.
- Whitmore, L.; Wallace, B. A. *Nucleic Acids Res.* 2004, **32**, W668-W673.
- Siddhuraju, P. *Food Chem.* 2006, **99**, 149-157.
- Yildirim, A.; Mavi, A.; Kara, A. A. *J. Agric. Food Chem.* 2001, **49**, 4083-4089.
- Wang, X.; Liu, F.; Liu, L.; Wei, Z.; Yuan, F.; Gao, Y. *Food Chem.* 2015, **173**, 564-568.
- Zhao, J.; Xiang, J.; Wei, T.; Yuan, F.; Gao, Y. *Food Res. Int.* 2014, **66**, 216-227.
- Yuan, Y.; Gao, Y.; Zhao, J.; Mao, L. *Food Res. Int.* 2008, **41**, 61-68.
- Kim, J. S.; Lee, Y. S. *Food Chem.*, 2009, **116**, 846-853.
- Sabir, M. A.; Sosulski, F. W.; Finlayson, A. J. *J. Agri. Food Chem.* 1974, **22**, 575-578.
- Spotti, M. J.; Perduca, M. J.; Piagentini, A.; Santiago, L. G.; Rubiolo, A. C.; Carrara, C. R. *Food Hydrocolloid*, 2013, **31**, 26-32.
- Lahtinen, S. J.; Knoblock, K.; Drakoularakou, A.; Jacob, M.; Stowell, J.; Gibson, G. R.; Ouwehand, A. C. *Biosci. Biotech. Bioch.* 2010, **74**, 2016-2021.
- Rizzarelli, P.; Carroccio, S. *Anal. Chim. Acta* 2014, **808**, 18-43.

## ARTICLE

RSC Advances

- 41 Almrhag, O.; George, P.; Bannikova, A.; Katopo, L.; Chaudhary, D.; Kasapis, S. *Food Chem.* **2012**, *134*, 1938-1946.
- 42 Wang, H.; Shi, Y.; Le, G. *Carbohydr. Polym.* 2014, **113**, 225-230.
- 43 Laroque, D.; Inisan, C.; Berger, C.; Vouland, É.; Dufossé, L.; Guérard, F. *Food Chem.* **2008**, *111*, 1032-1042.
- 44 Oliveira, F. C. D.; Coimbra, J. S. D. R.; de Oliveira, E. B.; Zuñiga, A. D. G.; Rojas, E. E. G. *Crit. Rev. Food Sci.* 2014, DOI:10.1080/10408398.2012.755669
- 45 Prigent, S. V.; Voragen, A. G.; Li, F.; Visser, A. J.; van Koningsveld, G. A.; Gruppen, H. *J. Sci. Food Agri.* 2008, **88**, 1748-1754.
- 46 Hashemi, M. M.; Aminlari, M.; Moosavinasab, M. *LWT-Food Sci. Technol.* 2014, **57**, 594-602.
- 47 Wang, W. Q.; Bao, Y. H.; Chen, Y. *Food Chem.* 2013, **139**, 355-361.
- 48 Bhattacharya, D.; Sahu, S. K.; Banerjee, I.; Das, M.; Mishra, D.; Maiti, T. K.; Pramanik, P. J. *Nanopart. Res.* 2011, **13**, 4173-4188.
- 49 Gu, F. L.; Kim, J. M.; Abbas, S.; Zhang, X. M.; Xia, S. Q.; Chen, Z. X. *Food Chem.* 2010, **120**, 505-511.
- 50 Zhu, K. X.; Sun, X. H.; Chen, Z. C.; Peng, W.; Qian, H. F.; Zhou, H. M. *Food Chem.* 2010, **123**, 1163-1169.
- 51 Yin, C.; Yang, L.; Zhao, H.; Li, C. P. *Food Res. Int.* 2014, **64**, 855-863.
- 52 Sun, Y.; Hayakawa, S.; Izumori, K. *J. Agric. Food Chem.* 2004, **52**, 1293-1299.
- 53 Liu, Y.; Zhao, G.; Zhao, M.; Ren, J.; Yang, B. *Food Chem.* 2012, **131**, 901-906.
- 54 Mangavel, C.; Barbot, J.; Popineau, Y.; Guéguen, J. J. *Agric. Food Chem.* 2001, **49**, 867-872.
- 55 Yang, W.; Liu, F.; Xu, C.; Yuan, F.; Gao, Y. *Food Res. Int.* 2014, **64**, 141-149.
- 56 Xia, S.; Li, Y.; Xia, Q.; Zhang, X.; Huang, Q. *Food Hydrocolloid*, 2015, **43**, 228-235.
- 57 Bengoechea, C.; Peinado, I.; McClements, D. J. *Food Hydrocolloid*, 2011, **25**, 1354-1360.
- 58 Miao, X.; Ling, L.; Shuai, X. *Chem. Commun.* 2011, **47**, 4192-4194.
- 59 Silván, J. M.; van de Lagemaat, J.; Olano, A.; del Castillo, M. D. J. *Pharmaceut. Biomed.* 2006, **41**, 1543-1551.
- 60 Rohn, S.; Rawel, H. M.; Kroll, J. *J. Agr. Food Chem.* **2004**, *52*, 4725-4729.
- 61 Shon, M. Y.; Kim, T. H.; Sung, N. J. *Food Chem.* 2003, **82**, 593-597.
- 62 Zhu, D.; Damodaran, S.; Lucey, J. A. *J. Agric. Food Chem.* 2010, **58**, 2988-2994.
- 63 Lei, F.; Liu, F.; Yuan, F.; Gao, Y. *Food Hydrocolloid*, 2014, **39**, 163-170.
- 64 Drusch, S.; Berg, S.; Scampicchio, M.; Serfert, Y.; Somoza, V.; Mannino, S. *Food Hydrocolloid*. 2009, **23**, 942-948.

**Table 1** Changes of second structures of LF, CA-LF conjugate and CA-LF- Glc/PD mixtures/conjugates.

Samples	$\alpha$ -Helix	$\beta$ -Sheet	$\beta$ -Turns	Unordered
LF	0.550	0.086	0.151	0.257
CA-LF con	0.385	0.086	0.226	0.320
CA-LF-Glc mix	0.561	0.084	0.126	0.248
CA-LF-Glc con	0.386	0.093	0.211	0.334
CA-LF-PD mix	0.527	0.090	0.159	0.271
CA-LF-PD con	0.336	0.087	0.248	0.356

**Table 2** Denaturation temperature ( $T_d$ ) and enthalpy change ( $\Delta H$ ) of LF, CA-LF conjugate and CA-LF-Glc/PD mixtures/conjugates at pH 7.0.

Samples	$T_{onset}$	$T_d$	$\Delta H$ (mJ/mg)
LF	63.57±0.12 (88.34±0.15)	68.43±0.23 (89.14±0.17)	-9.26±0.03 (-0.12±0.01)
CA-LF con	64.14±0.22	71.61±0.21	-2.87±0.06
CA-LF-Glc mix	68.53±0.19	68.72±0.09	-3.00±0.04
CA-LF-Glc con	69.87±0.13	72.13±0.14	-1.36±0.07
CA-LF-PD mix	68.10±0.23	74.03±0.20	-3.43±0.08
CA-LF-PD con	71.60±0.16	76.04±0.08	-1.66±0.03

**Figure captions**

**Figure 1** UV–Vis spectra (a), UV absorbance at 294 and 420 nm (b) and the content of free amino groups (c) of LF, CA-LF conjugate, CA-LF-Glc/PD mixtures and conjugates.

**Figure 2** MALDI-TOF-MS analysis of native/control LF, native/control CA-LF conjugates and CA-LF- Glc/PD conjugates.

**Figure 3** Proposed reactions of LF, CA and glucose/polydextrose. The quinone derivatives may be monomer, dimer, or polymer.

**Figure 4** FTIR spectra of LF, CA, CA-LF conjugate (a) and CA-LF-Glc/PD mixtures and conjugates (b).

**Figure 5** Far-UV CD (a) and fluorescence spectra (b) of LF, CA-LF conjugate, CA-LF-Glc/PD mixtures and conjugates.

**Figure 6** Atomic force microscopy images ( $2.0 \times 2.0 \mu\text{m}$ ) (a), particle size distribution (b) and  $\zeta$ -potential (c) of LF, CA-LF conjugate, CA-LF- Glc/PD mixtures and conjugates in solutions.

**Figure 7** Antioxidant activities of LF, CA, CA-LF conjugate, CA-LF-Glc/PD mixtures and conjugates (a)  $\text{ABTS}^{\bullet+}$  scavenging activity, (b) reducing power.

**Figure 8** The effect of processing condition (a)  $100\text{ }^{\circ}\text{C}$  for 5 min, (b) freeze-thaw treatment, (c) low pH and (d) high ionic strength on the particle size of  $\beta$ -carotene emulsions stabilized by LF, CA-LF conjugate, CA-LF-Glc/PD mixtures and conjugates.

**Figure 9**  $\beta$ -Carotene degradation as a function of storage time (a) at  $25\text{ }^{\circ}\text{C}$  and (b) at  $37\text{ }^{\circ}\text{C}$  in emulsions stabilized by LF, CA-LF conjugate, CA-LF-Glc/PD mixtures and conjugates.

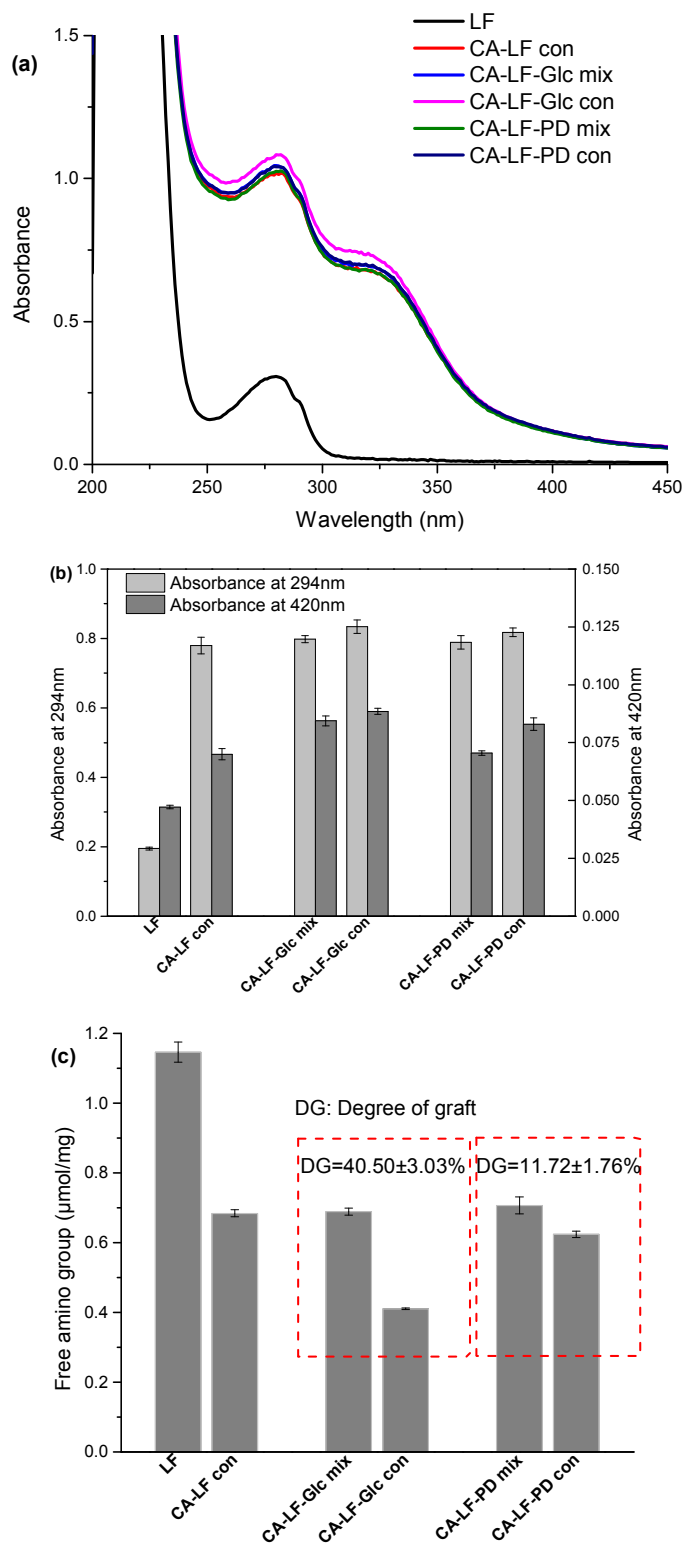


Fig. 1

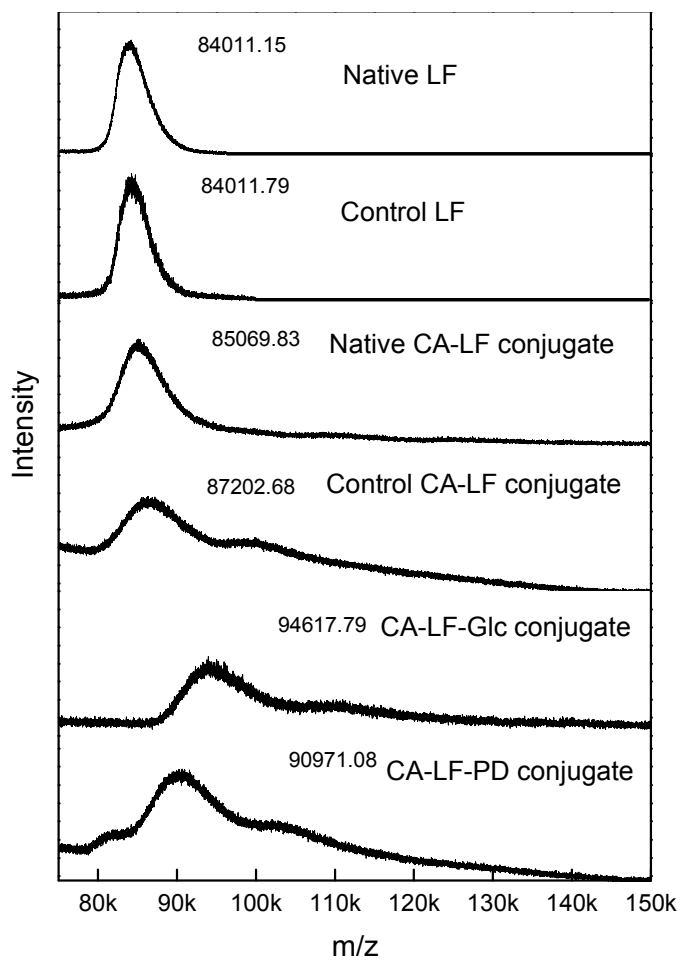


Fig. 2



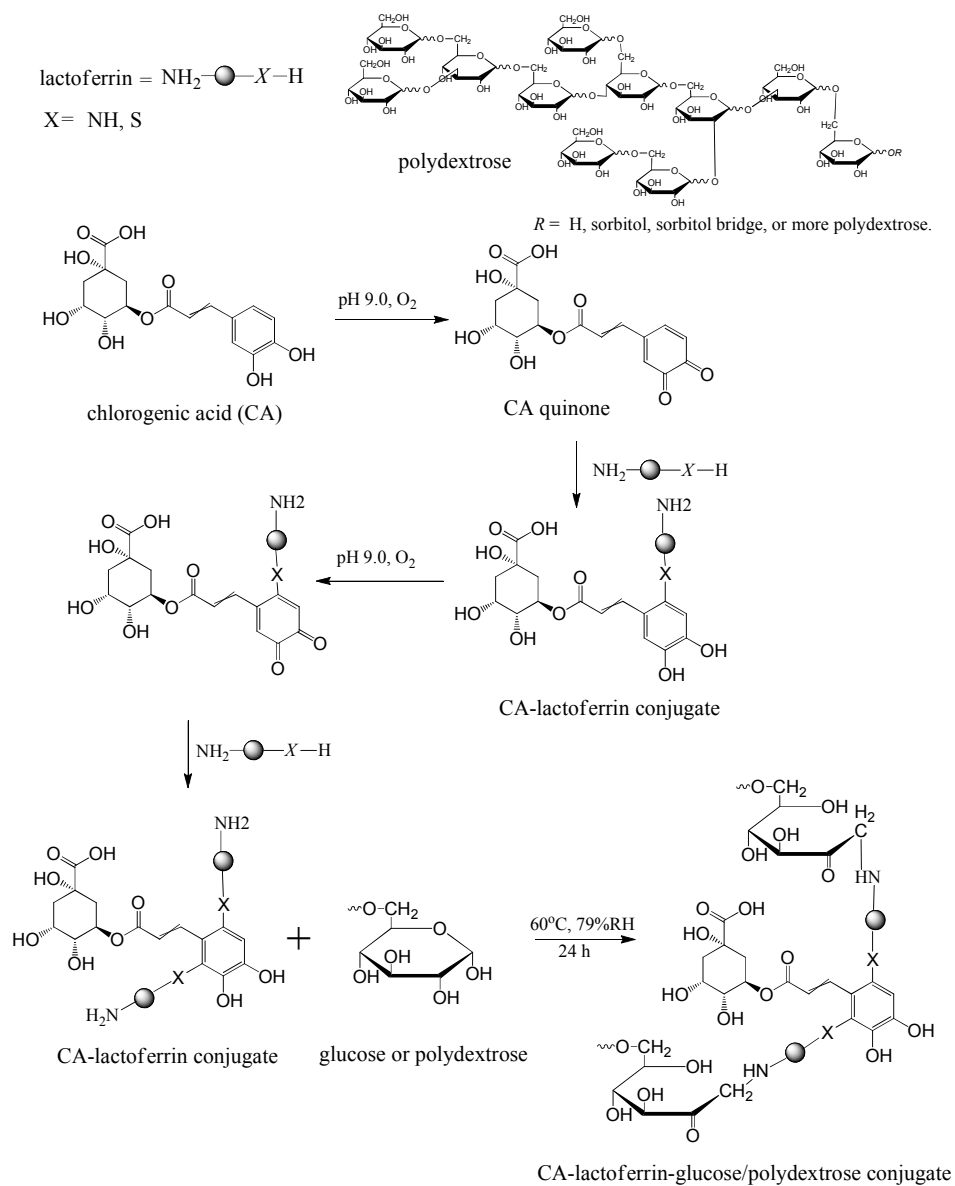
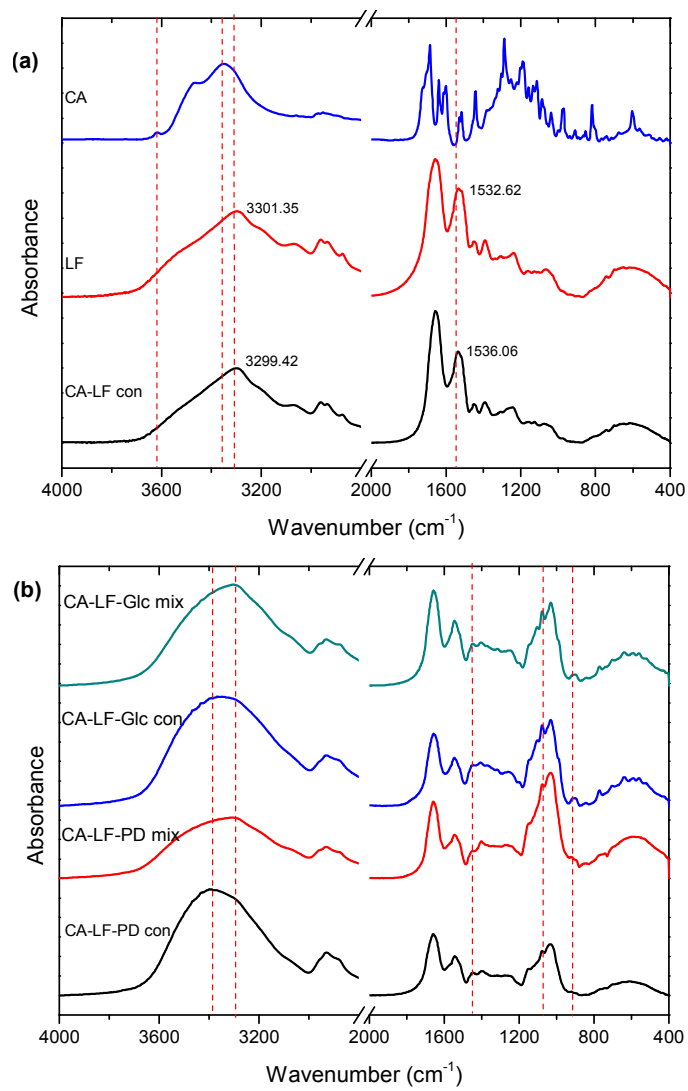


Fig. 3

**Fig. 4**

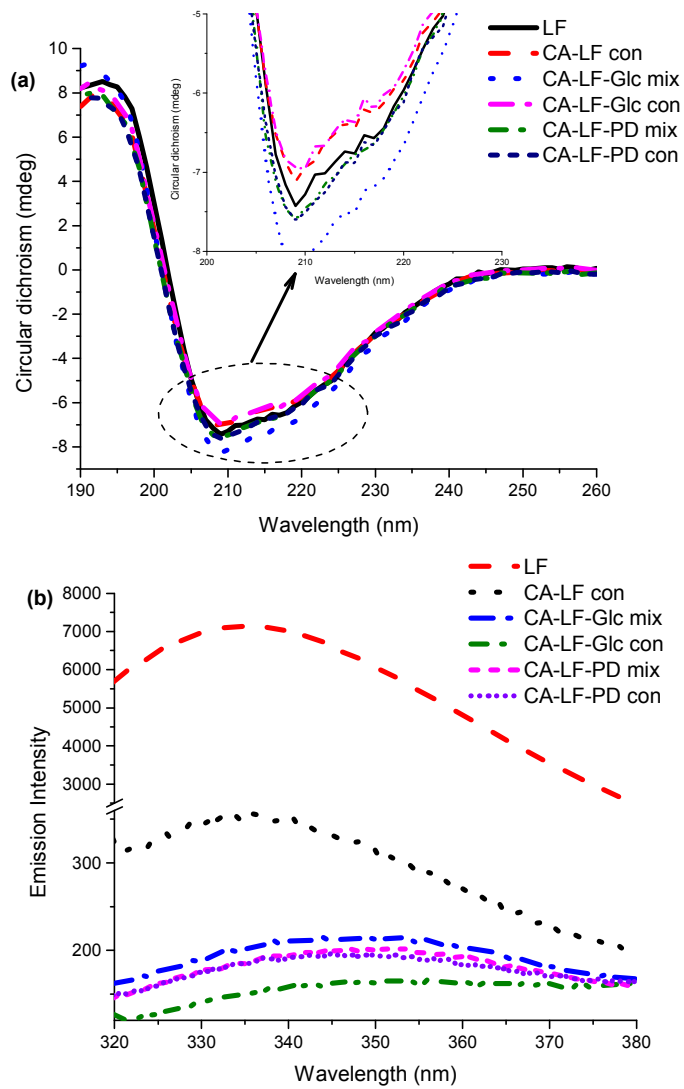


Fig. 5

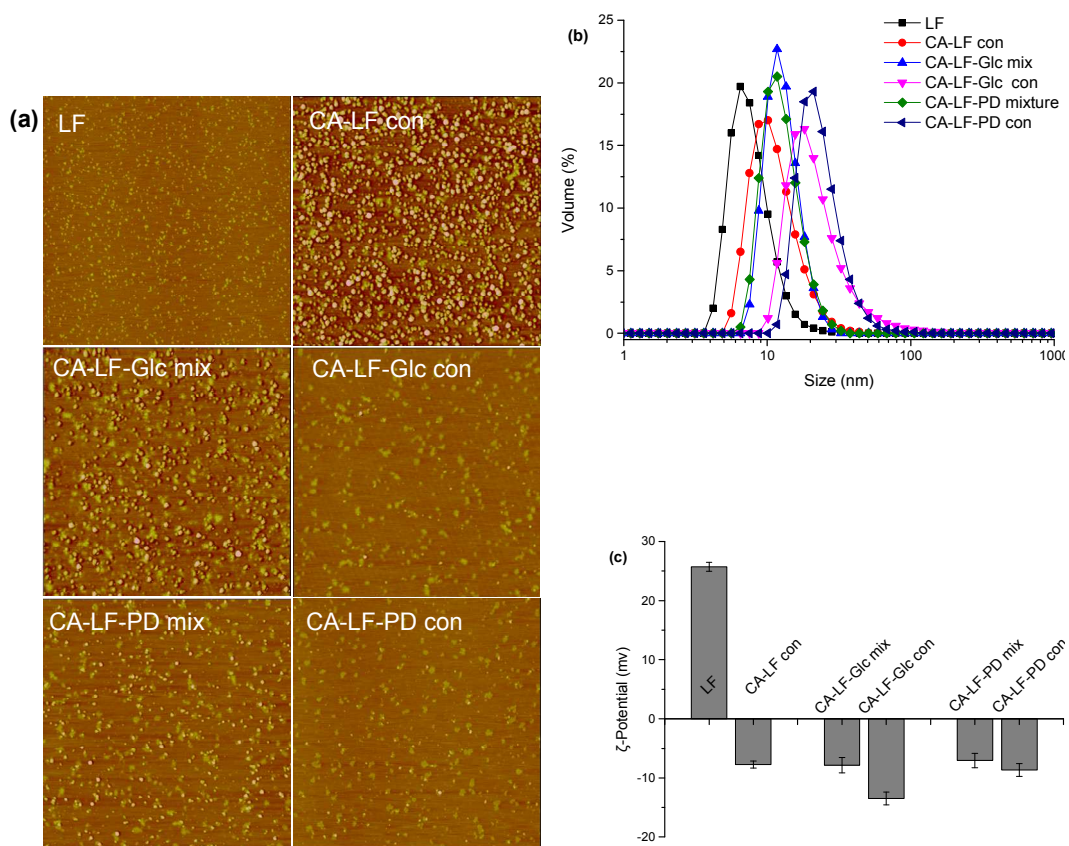


Fig. 6

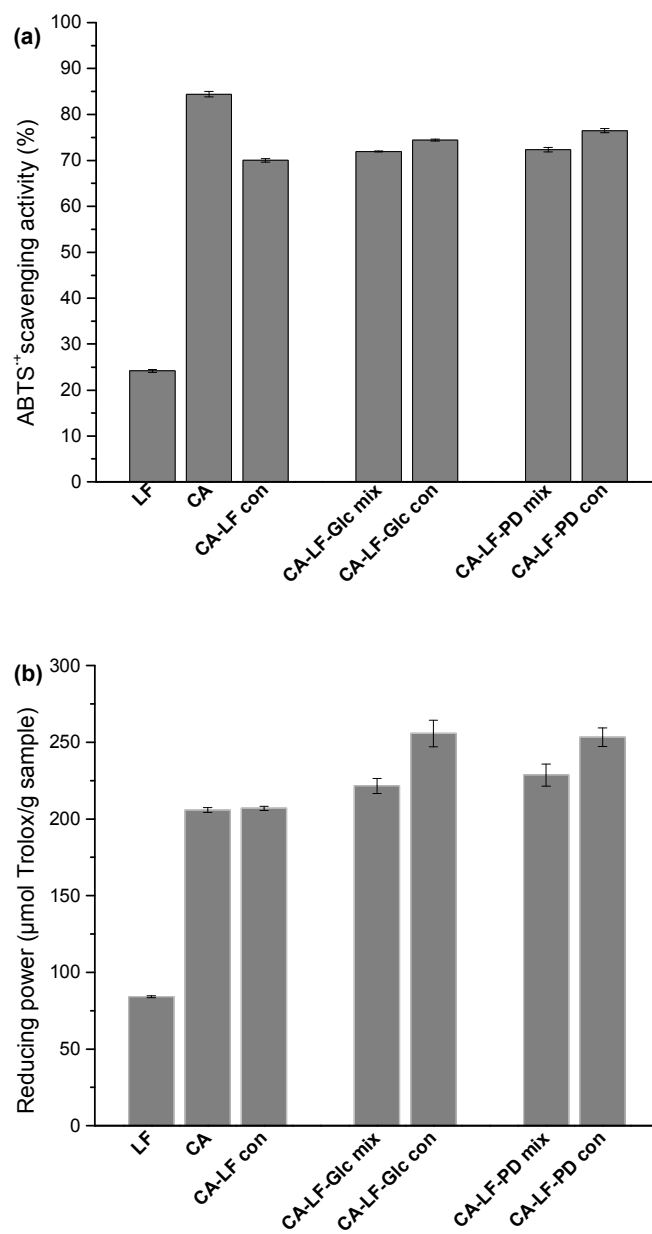


Fig. 7

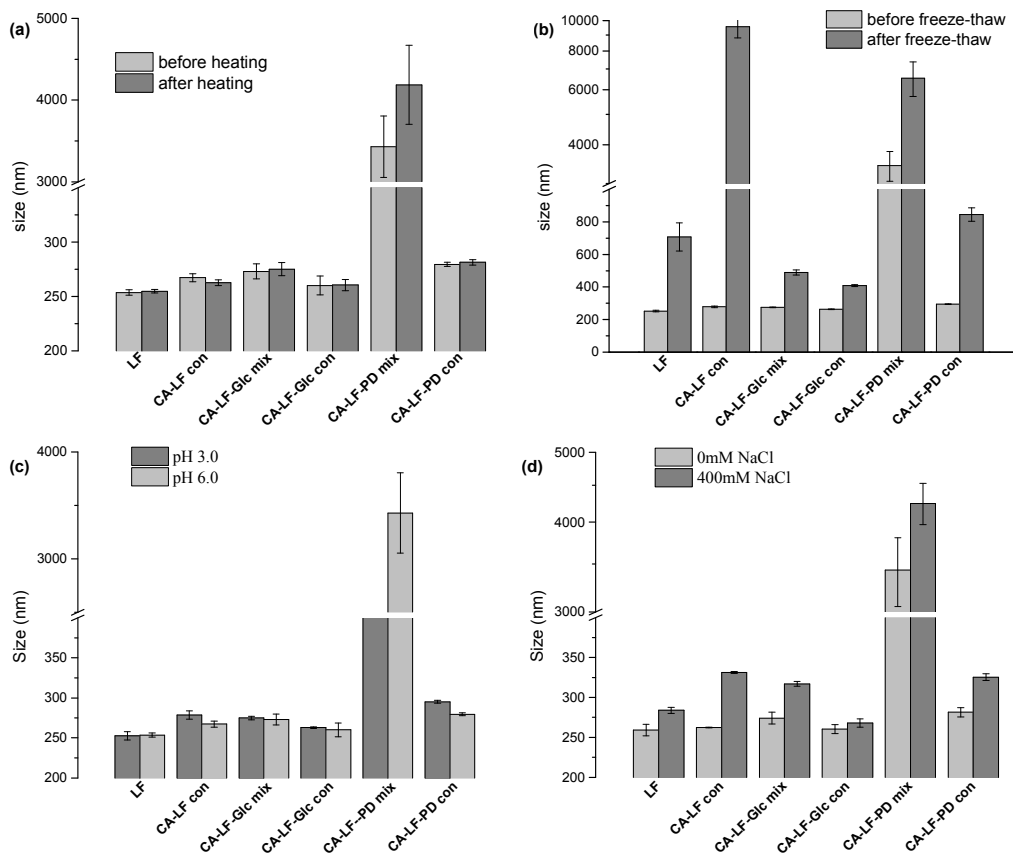
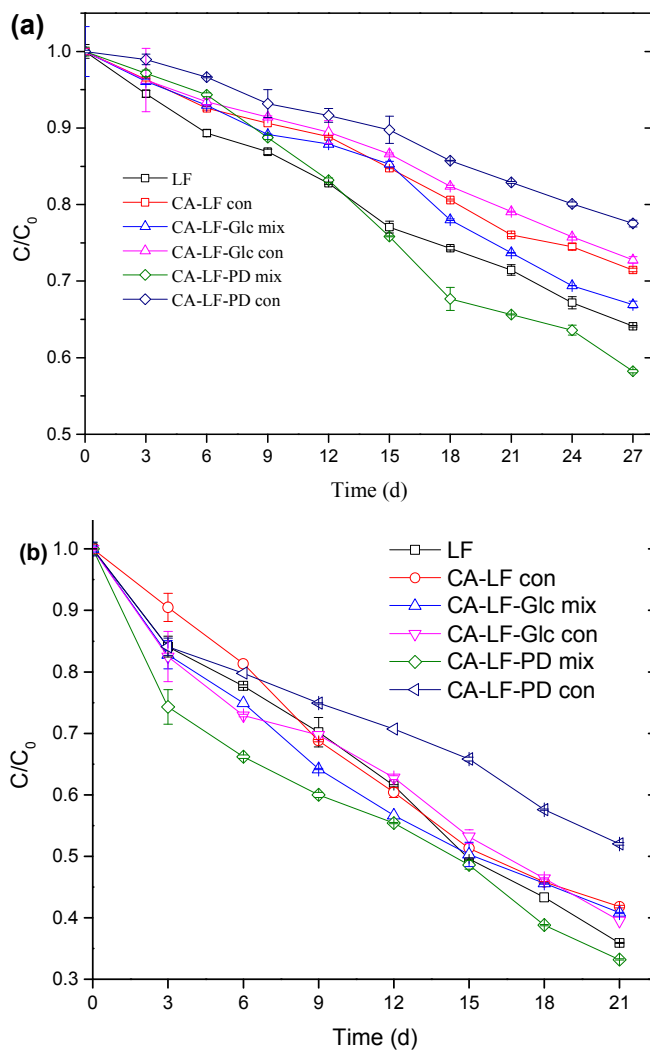


Fig. 8

**Fig. 9**